NeuroImage 102 (2014) 894–903

Contents lists available at ScienceDirect

NeuroImage

journal homepage: www.elsevier.com/locate/ynimg

# Local awakening: Regional reorganizations of brain oscillations after sleep ☆

Pei-Jung Tsai [a], Sharon Chia-Ju Chen [b], Chun-Yao Hsu [c], Changwei W. Wu [d,*], Yu-Chin Wu [e], Ching-Sui Hung [f], Albert C. Yang [g], Po-Yu Liu [h], Bharat Biswal [i], Ching-Po Lin [a]

[a] Department of Biomedical Imaging and Radiological Sciences, National Yang-Ming University, Taipei, Taiwan
[b] Department of Medical Imaging and Radiological Sciences, Kaohsiung Medical University, Kaohsiung, Taiwan
[c] Department of Psychiatry, Kaohsiung Medical University Chung-Ho Memorial Hospital, Kaohsiung, Taiwan
[d] Graduate Institute of Biomedical Engineering, National Central University, Taoyuan, Taiwan
[e] Department of Medical Imaging, Cheng Hsin General Hospital, Taipei, Taiwan
[f] Department of Research and Education, Taipei City Hospital, Taipei, Taiwan
[g] Department of Psychiatry, Taipei Veterans General Hospital, Taipei, Taiwan
[h] Department of Radiology, Hualien Armed Forces General Hospital, Hualien, Taiwan
[i] Department of Radiology, New Jersey Medical School, Newark, NJ, USA

ARTICLE INFO

*Article history:*
Accepted 18 July 2014
Available online 24 July 2014

*Keywords:*
Local sleep
Local awakening
Simultaneous EEG–fMRI recordings
Functional connectivity
Spectral power
Thalamo-cortical connectivity

ABSTRACT

Brain functions express rhythmic fluctuations accompanied by sleep and wakefulness each day, but how sleep regulates brain rhythms remains unclear. Following the dose-dependent local sleep concept, two succeeding questions emerge: (1) is the sleep regulation a network-specific process; and (2) is the awakening state dependent on the previous sleep stages? To answer the questions, we conducted simultaneous EEG and fMRI recordings over 22 healthy male participants, along pre-sleep, nocturnal sleep and awakening. Using paired comparisons between awakening and pre-sleep conditions, three scenarios of the regional specificity were demonstrated on awakening: (1) the default-mode and hippocampal networks maintained similar connectivity and spectral power; (2) the sensorimotor network presented reduced connectivity and spectral power; and (3) the thalamus demonstrated substantially enhanced connectivity to the neo-cortex with decreased spectral power. With regard to the stage effect, the deep sleep group had significant changes in both functional connectivity and spectral power on awakening, whereas the indices of light sleep group remained relatively quiescent after sleep. The phenomena implied that slow-wave sleep could be key to rebooting the BOLD fluctuations after sleep. In conclusion, the regional specificity and the stage effect were verified in support of the local awakening concept, indicating that sleep regulation leads to the reorganization of brain networks upon awakening.


## Introduction

Previous descriptions of sleep have recognized it as an offline period of consciousness. However, studies have shown that the simple dichotomy between sleep and wakefulness is invalid (Edgar et al., 1993; Steriade et al., 2001). From the neuroscience perspective, the literature suggests that sleep is not a quiescent offline state with minimal brain activities, but is composed of intensive variations of spatio-temporal oscillations across the brain (Dang-Vu et al., 2010; Massimini et al., 2005). The distributed oscillating signals originate from the spontaneous molecular process, internally transferring essential information, forming synaptic plasticity and network reorganization founded by multiple sleep stages (Adam and Oswald, 1977; Karni et al., 1994; Walker and Stickgold, 2006). Detected by electroencephalography (EEG) and polysonography, the sleep stages were believed to facilitate the reorganization and restoration of cerebral physiology (Aserinsky and Kleitman, 1953; Iber, 2007). The spontaneous propagation of these temporal features, such as spindles, slow-wave activities, and rapid eye movement (REM) activity, during sleep leads to the energy conservation and reorganization of attention and memory (Hu et al., 2006; Walker and Stickgold, 2006). Although researchers have made advances in understanding what occurs during sleep, how much sleep is optimal and how to measure sleep regulation become primary challenges for further sleep investigations (Roenneberg, 2013). Once determined, the sleep quality measurement can provide positive and pervasive benefits to most patients with sleep disorders, or even to the healthy public.

☆ Part of this work has been presented in 19th Annual Meeting of the Organization for Human Brain Mapping, 2013.

* Corresponding author at: Room S1-020, Science Bldg. 2, National Central University, Jhongli City, Taoyuan County 320, Taiwan.
*E-mail address:* restingfmri@gmail.com (C.W. Wu).

http://dx.doi.org/10.1016/j.neuroimage.2014.07.032
1053-8119/

Beyond investigating the intrinsic nature of sleep architecture, an alternative viewpoint for estimating sleep regulations is to detect the recovery condition after sleep (Hayashi et al., 2010; Voss, 2010). Awakening from sleep not only suggests the restoration of consciousness and body energy, but also reflects the synchronous integration of multiple neural assemblies (Mignot, 2008). Therefore, the brain activity on awakening has the potential to detect sleep efficiency and daytime arousal level (Hayashi et al., 2010; Jung et al., 2014). However, public attention on awakening remains focusing on the temporary decrement of subsequent cognitive performance immediately after sleep, or "sleep inertia" (Tassi and Muzet, 2000), so the importance of the awakening condition was underestimated. Ferrara observed an increased EEG power in the delta to low-alpha bands (1–9 Hz) and a decreased power in the beta range (18–24 Hz) on awakening (Ferrara et al., 2006). Marzano et al. confirmed an enhanced delta power in the posterior brain, reduced delta power in the frontal regions, and a generalized decrease of beta power on the overall scalp within 10 min after awakening (Marzano et al., 2011). These reports noted that brain functions on awakening possess regional specificity, implying the possibility of estimating sleep regulation effects on brain networks immediately after sleep.

Such regional specificity was also noted during sleep. The "local sleep" concept underpins that cortical activities during sleep reflect regional variations in brain activities while awake (Nir et al., 2011; Vyazovskiy et al., 2011). Huber reported that local slow-wave activity (SWA) distribution in the brain has high correlations with the learning-associated synapse connection before sleep (Huber et al., 2004). Hung demonstrated that under consecutive 24-h language and visuomotor tasks, slow/theta power (2–6 Hz) locally increased within the task-related brain regions (Hung et al., 2013), suggesting that previous waking experiences affect regional sleep patterns. Echoing the local sleep notion, a local awakening concept is founded in the current study with the following two postulations: (1) sleep regulation has regional specificity, imposing the reorganizations of brain dynamics before and after sleep, and (2) cortical activity or network synchrony on awakening is mediated by stage characteristics during sleep. Previously, Ikeda and Hayashi detected arousal-level disparities existing between various task performances on awakening, providing a preliminary evidence for local awakening (Ikeda and Hayashi, 2008). For spatial reorganization, Balkin reported a possible shift in regional cerebral blood flow (rCBF) and brain interregional connectivity after awakening (Balkin et al., 2002). Though previous studies implied the regional changes upon awakening, the specific impact on the brain networks and the link between the awakening condition and the previous sleep contents remain question marks. Therefore, as the first trial to test the local awakening concept, we tested the regional specificity across networks and whether the existence of the slow-wave sleep affects the following awakening condition across local brain networks.

In the current study, two steps were adopted to test the hypothesis and the local awakening concept. The first step is to measure the regional changes of brain dynamics before and after sleep using the resting-state functional magnetic resonance imaging (RS-fMRI) technology for the 2 advantages (Biswal et al., 1995). First, the RS-fMRI technique measures the dynamic disparities across multiple brain networks within a single session (Biswal et al., 2003; Yang et al., 2007). Second, because participants are unable to respond to external stimuli during sleep (Larson-Prior et al., 2009; Sämann et al., 2011), the RS-fMRI technique is suitable for observing transient brain interactions associated with sleep while providing high spatial resolution. In practice, we measured both spectral power and interregional synchronizations before and after sleep across multiple sleep-related brain networks, including the default-mode network (Horovitz et al., 2009; Sämann et al., 2011), the sensorimotor network (Larson-Prior et al., 2009), the hippocampal network (Hu et al., 2006; Walker and Stickgold, 2006) and thalamo-cortical networks (Boveroux et al., 2010). The second step is to test the causal effect of previous stage-3 (N3) sleep on the awakening brain. We segregated the participants into 2 groups, with and without N3 sleep, and observed their BOLD spectral power and functional connectivity for how sleep architecture modulates cerebral organizations on awakening.

## Materials and methods

### *Participant preparation*

We recruited 22 healthy men with regular sleep duration of 7–8 h per night, with consistent bed/wake times for at least 4 days. They had no daytime nap habits, no excessive daytime sleepiness, and no history of neurological or psychiatric disorders. Participant ages ranged from 20 to 39 years (mean $\pm$ std $= 23.8 \pm 4.2$ years). The participants were requested not to consume alcohol or caffeine-containing foods or drinks on the day of the experiment. Before scanning, we requested the participants to complete the Pittsburgh Sleep Quality Index (PSQI), including sleep quality, duration and efficiency, to testify their sleep quality within the previous month. Informed consent was obtained from all participants prior to the experiments in accordance with the protocol approved by the Institutional Review Board of National Yang-Ming University.

### *Simultaneous EEG/fMRI recordings*

We conducted simultaneous EEG–fMRI recordings for each functional scan. The EEGs were recorded using a 32-channel MR-compatible system (Brain Products, Gilching, Germany). The 32 electrodes, including 30 EEG channels, one electrooculography (EOG) channel, and one electrocardiogram (ECG) channel, were positioned according to the international 10/20 systems. The built-in impedance in each electrode was 5 kΩ and the electrode-skin impedance was reduced under 5 kΩ using abrasive electrode paste (ABRALYT HiCl). The EEG signal was synchronized with the MR trigger and recorded using Brain Vision Recorder software (Brain Products) with a 5 kHz sampling rate and a 0.1 μV voltage resolution. A low-pass and a high-pass filter were set at 250 Hz and 0.0159 Hz, respectively, with an additional 60-Hz notch filter. MRI data were acquired using a 3T Siemens Tim Trio system (Erlangen, Germany) using a 12-channel head coil. High-resolution T1-weighted anatomical images (3D-MPRAGE with $192 \times 192 \times 176$ matrix size, 1 $mm^3$ isotropic cube, flip angle (FA) $= 9°$ repeat time (TR) $= 1900$ ms, echo time (TE) $= 2.28$ ms, and inverse time (TI) $=$ 900 ms) were acquired prior to functional scans for geometric localization. Head motion was minimized using customized cushions. Functional scans were subsequently acquired using a single-shot, gradient-recalled echo planar imaging (EPI) sequence (TR/TE/FA $= 2500$ ms/30 ms/80°, field of view $= 220$ mm, matrix size $= 64 \times 64$, 35 slices with 3.4 mm thickness) aligned along the AC–PC line, allowing whole-brain coverage.

The experimental protocol was conducted between 11 pm and 4 am. After EEG preparation, the participants were tied with a pneumatic belt and an oximeter for simultaneous recordings of respiration and cardiac pulsations. At the onset of the MR scan, the T1-weighted anatomical images were acquired for 5.5 min. The simultaneous EEG/fMRI datasets were subsequently recorded for 3 sessions: (1) ***Pre-sleep*** *session*: the participants were instructed to remain in a resting state with their eyes closed, awake, maintaining their head position, and not thinking of anything particular, for 6 min (144 scans) before the *Sleeping* session. (2) **Sleeping** *session*: Participants were instructed to fall asleep after the scan started. Two criteria were used to terminate this session. First, the scan terminated at 125 min primarily because of hardware stability. Second, participants who were unable to fall asleep for a longer period could report their willingness to terminate this session. (3) **Awakening** *session*: Subsequent to the *Sleeping* session, the *Awakening* session repeated the protocol of the *Pre-sleep* session, resting for another 6 min without falling asleep.

*Data preprocessing*

Recorded EEG data was preprocessed offline using Analyzer 2.0 (Brain Products). Four electrodes (C3, C4, O1, and O2) were used to determine the sleep stages. The preprocess included down-sampling the EEG signal to 250 Hz, removing the gradient-induced artifact (adaptive average subtraction) and removing the ballistocardiographic artifact using the algorithm based on the R–R interval estimation from the ECG electrode. We primarily used EEG recordings for sleep scoring to ensure sleep efficiency in the *Sleeping* session and the arousal level in both *Pre-sleep* and *Awakening* sessions. A licensed sleep technician from Kaohsiung Medical University Hospital visually scored the sleep stages (N1, N2, N3, and REM sleep) from the EEG data for every 30-s epoch, according to the current criteria of the American Academy of Sleep Medicine (AASM) (Iber, 2007). All fMRI data were preprocessed by Statistical Parametric Mapping (SPM5; Wellcome Institute of Cognitive Neurology, University College London, London, UK). Functional connectivity and fluctuation analyses were accomplished using REST (Song et al., 2011) and AFNI (Cox, 1996). In the preprocessing stage, the first 4 volumes of each session were discarded for achieving steady state before conducting realignment using rigid body transformation for correcting head motion (*Inline Supplementary Table S1*). The fMRI datasets were spatially normalized to a standard Montreal Neurological Institute (MNI) template, resampled to an isotropic resolution of $2 \times 2 \times 2$ mm$^3$, and smoothed with a Gaussian kernel (FWHM = 6 mm) for improving the signal-to-noise ratio. Then the linear detrending was applied to eliminate signal drift induced by system instability. Finally, the effects of nuisance regressors, including the six motion parameters, respiration/cardiac pulsations, white matter and cerebrospinal fluid signals, were removed from all preprocessed datasets.

Inline Supplementary Table S1 can be found online at http://dx.doi.org/10.1016/j.neuroimage.2014.07.032.

*Functional connectivity analysis*

To examine the inter-regional connectivity on awakening, seed-based correlation analysis was performed on both *Pre-sleep* and *Awakening* sessions, and then a band-pass filter (0.01–0.1 Hz) was applied to all datasets. Four spherical seeds (3 mm in radius) were subsequently assigned to access functional networks associated with sleep (van Dijk et al., 2010): (1) Right primary motor cortex (M1) [36, −25, 57] for the sensorimotor network (in the MNI coordinate); (2) right posterior cingulate cortex (PCC) [4, −53, 26] for the default-mode network; (3) right hippocampus (HPC) [24, −20, −22] for the hippocampal network; and (4) the bilateral medial thalamus (THA) [2, −14, 6] for the thalamo-cortical network. Then the average time courses were extracted from each seed on all participants, and the voxel-wise correlation coefficients were calculated between the seed time course and the time series of every other voxel in the brain. The resulting correlation maps were transformed to z maps using Fisher's z transform. Group comparisons between *Pre-sleep* and *Awakening* sessions were conducted based on random effect (FWE-corrected $P < .01$ for single-session results and FDR-corrected $P < .01$ for between-session comparison).

Additionally, we applied region of interest (ROI) analysis to evaluate sleep regulation effect. The following 10 ROIs were adopted from the Automated Anatomical Labeling (AAL) template (Tzourio-Mazoyer et al., 2002) to prevent the manipulative bias. In SMN, ROIs included bilateral M1 (M1R and M1L), supplementary motor area (SMA) and postcentral sensory area (SSR). In default-mode network (DMN) and hippocampal network (HPN), we included PCC, anterior cingulate cortex (ACC), bilateral angular gyri (AG), middle temporal cortices (MT) and HPC. Extra regions of the middle cingulum (MCC) and the calcarine area (VIS) were chosen for thalamo-cortical connectivity.

*Spectral power analysis*

Because sleep modulates baseline hemodynamics (Balkin et al., 2002; Kuboyama et al., 1997), we compared the low-frequency blood oxygenation level dependent (BOLD) fluctuations before and after sleep and included 2 spectral analyses: (1) the voxel-based amplitude of low-frequency fluctuations (ALFF) to locate the affected brain regions (Yang et al., 2007), and (2) the ROI-based Fourier transform to locate the impacted frequency ranges. The ALFF analysis was conducted using the voxel-wise Fourier transform, and the square root of the power spectrum across 0.01–0.1 Hz was regarded as the ALFF index. For compensating the global variations in the whole brain, the normalized ALFF (ALFFn) was defined as dividing the voxel-wise ALFF by the average ALFF of the entire brain, subtracted by unity. The positive ALFFn indicates higher fluctuation amplitude than the global ALFF within the observant frequency range. In the group analysis, we conducted the one-sample t-test on the ALFF/ALFFn maps for each session and then performed a paired t-test for between-session comparison (FDR-corrected $P < .01$). Besides, the ROI-based spectrum analysis was conducted on the preprocessed datasets from both the *Pre-sleep* and *Awakening* sessions, within the same 10 ROIs as in the connectivity analysis for spectral evaluations. The time courses extracted from selective ROIs were baseline-removed and then transformed to the frequency domain. The average spectrum across participants represented power spectral density for each frequency bin (frequency range = 0–0.2 Hz; spectral resolution = 0.0028 Hz). In the group-level analysis, we conducted a paired comparison ($P < .01$) on the average spectral power between both sessions to localize frequency changes.

*Group segregation: awakening with and without N3 sleep*

Sleep inside the MR scanner was a novel experience for normal participants, which might have affected their sleep quality. Therefore, we listed sleep metrics (PSQI, total sleep time, pre-awakening stage, and sleep efficiency) and calculated the cross-correlation between each pair. To test whether sleep stages have causal effects on brain dynamics upon awakening, we segregated the 22 participants into 2 groups: 12 participants with N3 sleep (deep-sleep) and 10 participants without N3 sleep (light-sleep). The deep-sleep group was defined according to the criterion: participants had N3 sleep for over 5 min within the *Sleeping* session. The between-group comparison was also performed by voxel-wise functional connectivity analysis and ALFF analyses. The spectral power and connectivity strengths were then extracted from all AAL ROIs to identify significant changes in both connectivity and ALFF.

Across the entire article, we held 3 statistical criteria for all analyses: (1) one-sample t-test with FWE corrected $P < .01$ for the single group voxel-wise results, (2) paired t-test with FDR-corrected $P < .01$ for the repeated measure voxel-wise comparison, and (3) two-tailed t-test with $P < .01$ in the ROI analysis.

## Results

*Sleep scoring and architecture*

We scored EEG data into wake, N1, N2, N3, and REM sleep. All participants reached N2 sleep in the *Sleeping* session, and the individual sleep characteristics are summarized in Table 1. Among them, 18 reported self-awakening during the *Sleeping* session, and 4 who reached the maximum scan time (125 min) were forced to wake up. In addition, 12 participants had N3 sleep longer than 5 min, and 10 had sleep without sufficient N3 sleep. On average, the participants spent 30.9% in N1, 41.6% in N2, 12.5% in N3 sleep, and 3.2% in REM sleep. The total sleep time was 76.7 min inside the scanner and the overall sleep efficiency was 81.7%. Among the sleep characteristics, the total sleep time (TST) showed a significant positive correlation with sleep efficiency ($r = 0.85$, $P < .01$) and a

**Table 1**
Individual sleep scoring and sleep characteristics (unit: minutes).

| ID | PSQI | Wake | | N1 | | N2 | | N3 | | REM | | TRT | TST | SE |
|---|---|---|---|---|---|---|---|---|---|---|---|---|---|---|
| | | Time | (%) | Time | (%) | Time | (%) | Time | (%) | Time | (%) | Time | Time | (%) |
| 1 | 4 | 11.5 | (29) | 17 | (44) | 10.5 | (27) | | | | | 39 | 27.5 | (71) |
| 2 | 6 | 16.5 | (18) | 23.5 | (26) | 41 | (46) | 8.5 | (10) | | | 89.5 | 73 | (82) |
| 3 | 4 | 13.5 | (11) | 27 | (22) | 66.5 | (53) | 18.5 | (15) | | | 125.5 | 112 | (89) |
| 4 | 4 | 46.5 | (56) | 20.5 | (25) | 15.5 | (19) | | | | | 82.5 | 36 | (44) |
| 5 | 4 | 3.5 | (3) | 16.5 | (16) | 69 | (67) | 13.5 | (13) | | | 102.5 | 99 | (97) |
| 6 | 3 | 0 | (0) | 13.5 | (11) | 82 | (67) | 27.5 | (22) | | | 123 | 123 | (100) |
| 7 | 7 | 26 | (53) | 11.5 | (23) | 11 | (22) | 0.5 | (1) | | | 49 | 23 | (47) |
| 8 | 9 | 15.5 | (21) | 13.5 | (18) | 31.5 | (43) | 13 | (18) | | | 73.5 | 58 | (79) |
| 9 | 9 | 14 | (25) | 16 | (28) | 17.5 | (31) | 9.5 | (17) | | | 57 | 43 | (75) |
| 10 | 9 | 32 | (48) | 5.5 | (8) | 13.5 | (20) | 15 | (23) | | | 66 | 34 | (52) |
| 11 | 6 | 11.5 | (29) | 24.5 | (63) | 3 | (8) | | | | | 39 | 27.5 | (71) |
| 12 | 8 | 9 | (11) | 36.5 | (45) | 35 | (43) | | | | | 80.5 | 71.5 | (89) |
| 13 | 5 | 8 | (9) | 25.5 | (29) | 36.5 | (41) | 18 | (20) | | | 88 | 80 | (91) |
| 14 | 9 | 4.5 | (5) | 26 | (31) | 51 | (61) | 2 | (2) | | | 83.5 | 79 | (95) |
| 15 | 6 | 0.5 | (0) | 37.5 | (30) | 76 | (61) | 7.5 | (6) | 4 | (3) | 125.5 | 125 | (100) |
| 16 | 2 | 18.5 | (21) | 24 | (27) | 41 | (49) | 1 | (1) | 3 | (3) | 87.5 | 69 | (79) |
| 17 | 7 | 12 | (16) | 33 | (44) | 21 | (28) | 7.5 | (10) | 2 | (3) | 75.5 | 63.5 | (84) |
| 18 | 4 | 0 | (0) | 32 | (26) | 80.5 | (64) | 11.5 | (9) | 1 | (1) | 125 | 125 | (100) |
| 19 | 4 | 4.5 | (4) | 33.5 | (27) | 62 | (49) | 25.5 | (20) | | | 125.5 | 121 | (96) |
| 20 | 5 | 25.5 | (21) | 54 | (45) | 34 | (28) | | | 7 | (6) | 120.5 | 95 | (79) |
| 21 | 4 | 11 | (9) | 46 | (37) | 68.5 | (55) | | | | | 125.5 | 114.5 | (91) |
| 22 | 4 | 11 | (11) | 54.5 | (55) | 34 | (34) | | | | | 99.5 | 88.5 | (89) |
| Mean | 5.6 | 13.4 | (18.2) | 26.9 | (30.9) | 40.9 | (41.6) | 11.9 | (12.5) | 3.4 | (3.2) | 90.1 | 76.7 | (81.7) |

TRT = total recording time.
TST = total sleep time.
SE = TST/TRT for sleep efficiency.

negative correlation with PSQI ($r = -0.45$, $P < .05$). Beyond the *Sleeping* session, both *Pre-sleep* and *Awakening* sessions were scored for comparison as well. We found that 20 participants fell into N1/N2 sleep in the *Pre-sleep* session and 13 participants fell into N1 sleep in the *Awakening* session (*Inline Supplementary Table S2*). Even though, the factor did not conflict with our purpose because of two reasons. First, we aimed at testing the sleep regulation effect transforming from the sleepy condition (*Pre-sleep*) to the arousal condition (*Awakening*), which was with higher sleep pressure and deviant from the normal resting state. In contrast to *Pre-sleep*, the percentage of NREM sleep was significantly reduced in *Awakening* ($P < .002$), indicating reduced sleep pressure after the long-term *Sleeping* session. Second, under high sleep pressure at midnight, it is highly possible to score into NREM sleep due to signatures for micro-sleep when the subjects stay awake (Taillard et al., 2003). Therefore, we reserved all datasets to study the sleep regulation from *Pre-sleep* to *Awakening*.

Inline Supplementary Table S2 can be found online at http://dx.doi.org/10.1016/j.neuroimage.2014.07.032.

### *Functional connectivity of 3 cortical networks on awakening*

Fig. 1 illustrates group-level connectivity comparisons between *Pre-sleep* and *Awakening* on 3 networks: the sensorimotor network (SMN), the default-mode network (DMN), and the hippocampal network (HPN). In the SMN, bilateral M1 and SMA had strong connectivity before sleep (Fig. 1A upper panel, FWE-corrected $P < .01$); however, these connections shrank on awakening (Fig. 1A middle panel). The paired t-test comparison demonstrated (Fig. 1A lower panel, FDR-corrected $P < .01$) reduced SMN connectivity after sleep and enhanced connections to the thalamus. ROI analysis (Fig. 1D left panel) showed that z scores in SMN-related regions significantly decreased after sleep, and M1-THA connectivity turned from negative to positive ($P < .01$). In DMN, PCC (seed) was stably connected to MT, AG, and HPC in both *Pre-sleep* and *Awakening* sessions, whereas its connection to ACC increased slightly in the *Awakening* condition (Fig. 1B upper and middle panel). Between-session comparison (Fig. 1B lower panel) showed that only the connectivity to the medial thalamus was enhanced after sleep, whereas PCC–ACC connection was also enhanced in the ROI results (Fig. 1D middle panel). In HPN, the connections between bilateral HPC slightly increased after sleep, the hippocampal connection to the medial thalamus (Fig. 1C lower panel) was significantly enhanced on awakening. The contrast maps in Figs. 1A, B, and C shared a common phenomenon: the medial uncorrelated or anti-correlated thalamo-cortical synchronizations before sleep transformed to a positive correlation on awakening ($P < .01$). Cluster information is listed in Inline *Supplementary Table S3* and more detail connectivity results are shown in *Inline Supplementary Fig. S1*.

Inline Supplementary Table S3 can be found online at http://dx.doi.org/10.1016/j.neuroimage.2014.07.032.

Inline Supplementary Fig. S1 can be found online at http://dx.doi.org/10.1016/j.neuroimage.2014.07.032.

### *Spectral variability of 3 cortical networks on awakening*

Fig. 2 demonstrates the ALFF changes on awakening compared with *Pre-sleep*. The group-level comparison of ALFF maps (Fig. 2A upper panel) demonstrated that ALFF on awakening decreased in the posterior brain, particularly in the parietal and occipital lobes. Compared with the average ALFF across the entire brain, ALFFn (Fig. 2A lower panel) revealed that the prefrontal lobe and the subcortical regions possessed relatively strong fluctuations after sleep, while the posterior brain had decreased fluctuation amplitudes. Fig. 2B demonstrates the ALFF variability across ROIs in the 4 networks. Most ALFF values in DMN and HPN were higher than the identity line (identical ALFF across both sessions) except the thalamus, while ALFF values in SMN and THA were lower than the identity line, confirming the reduced ALFF in the posterior regions after sleep at the ROI level.

### *Thalamus spectral power and thalamo-cortical connectivity on awakening*

Fig. 3A shows the THA connectivity maps in both *Pre-sleep* and *Awakening* conditions (one sample t-test, FWE-corrected $P < .01$), and the contrast map between conditions (paired t-test, FDR-corrected $P < .01$). Under the same threshold, the connections from the thalamus to most

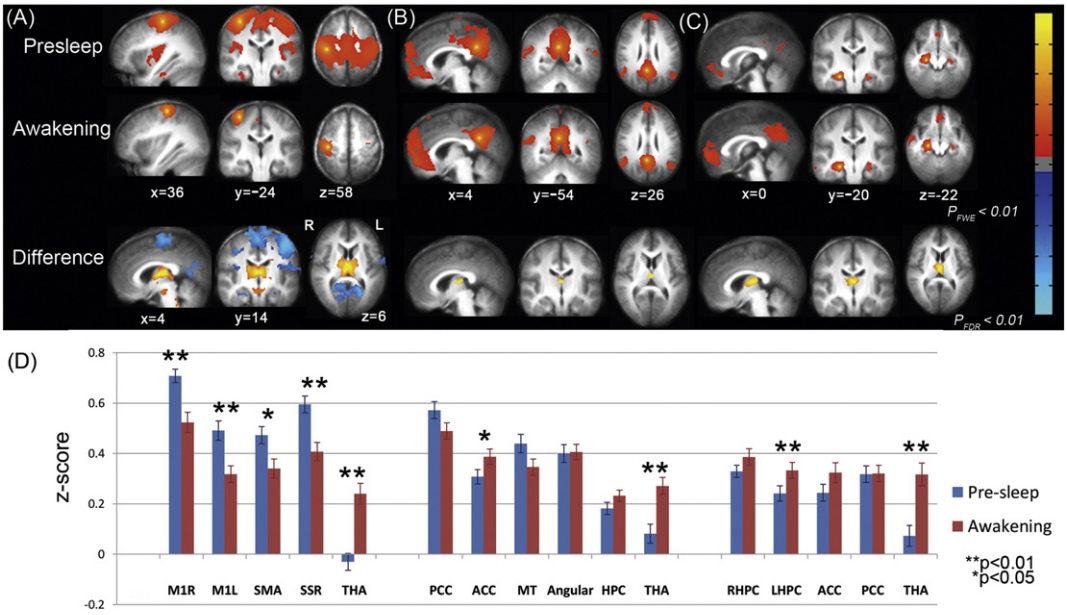


**Fig. 1.** Comparison of functional connectivity in 3 networks between *Pre-sleep* and *Awakening*. Brain maps represent one-sample group results in *Pre-sleep* (upper panel, FWE-corrected $P < .01$) and *Awakening* (middle panel), and the paired-comparison (lower panel, FDR-corrected $P < .01$) of the following networks: (A) sensorimotor, (B) default-mode, and (C) hippocampal networks. The warm color demonstrates a positive correlation (*Pre-sleep* and *Awakening*) or connectivity increase after sleep (contrast map), whereas the blue color shows a negative correlation or decrease after sleep. (D) ROI-based connectivity comparison in the 3 networks between *Pre-sleep* (blue) and *Awakening* (red) conditions ($^{*}P < .05$ and $^{**}P < .01$).

of the neocortex, cerebellum, and brain stem remarkably enhanced on awakening. Fig. 3B provides the ROI-based connectivity comparison between *Pre-sleep* and *Awakening* conditions ($P < .01$), denoting a global elevation of thalamo-cortical connectivity on awakening. Fig. 3D demonstrates that the THA waveform had relatively strong fluctuation ($\sigma = 5.40$) and weak anti-correlation ($r = -0.16$) with the M1 waveform (selected from the right anti-correlated region in the *Pre-sleep* session) in the *Pre-sleep* session; however, after sleep, their temporal relationship transformed to a positive correlation ($r = 0.46$) with reduced fluctuation amplitudes ($\sigma = 3.41$). Targeting on the medial thalamus (the common region of Fig. 1 difference maps in the 3 networks), Fig. 3C shows the significantly reduced THA spectral power (green highlights, paired t-test, $P < .01$) within 0.05–0.09 Hz on awakening.

*Stage effect on ROI-based functional connectivity and spectral power*

The interactions between sleep metrics and the changes of brain oscillations were evaluated using the ROI analysis. Upon awakening, the THA–VIS connection showed a positive correlation with TST ($r = 0.562$, $P < .05$) and N2 percentage ($r = 0.558$, $P < .05$). There were no interactions between sleep metrics and ALFF, but the ALFFn changes in HPC had positive correlation with pre-awakening stage ($r = 0.605$, $P < .05$). The detail interactions between sleep metrics and brain oscillation indices are listed in Table S4. A subsequent 2-sample comparison between the light-sleep and deep-sleep groups confirmed no significant difference in sleep metrics, ALFF and functional connectivity ($P > .3$ *for sleep metrics*, $P > .25$ for ALFF and $P > .06$ for FC) before sleep.

Among the observable networks, both groups showed reduced sensorimotor connectivity and enhanced thalamo-hippocampal connectivity on awakening (*Inline Supplementary Fig. S2A*). In ALFF, the deep sleep group demonstrated stronger reduction of spectral power in the visual/sensorimotor networks on awakening, whereas the light sleep group presented similar spectral power in both *Pre-sleep* and *Awakening*. However, the between-group difference did not pass the statistical threshold in both connectivity and ALFF maps (FDR-corrected $P > .3$, *Inline Supplementary Fig. S2B*). AAL-based between-condition comparisons are listed in Table S5. To further address the frequency specificity, we analyzed the power spectral density across 10 representative ROIs. Fig. 4 demonstrates the power spectra of *Pre-sleep* (blue) and *Awakening* (red) sessions in both light-sleep (upper panel) and deep-sleep (lower panel) groups. Reduced low-frequency power was particularly prominent in the deep-sleep group, and also the declined cross-subject variance was observed after sleep. Regarding the affected frequency range, the deep-sleep group showed significantly reduced power on awakening in M1 (0.01–0.07, 0.14–0.16 and 0.18–0.19), SMA (0.15–0.19 Hz), PCC (0.01–0.04, 0.07–0.08 and 0.13–0.16 Hz), VIS (almost across the

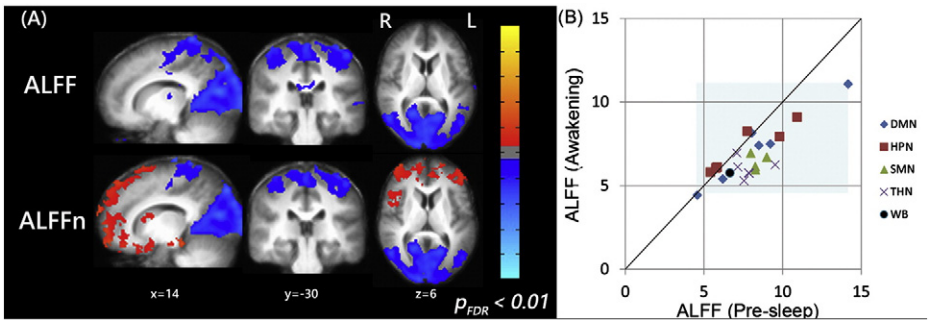


**Fig. 2.** (A) Paired comparison (FDR-corrected $P < .01$) of ALFF and normalized ALFF (ALFFn) maps between *Pre-sleep* and *Awakening*; and (B) scatter distribution of ALFF scores under *Pre-sleep* and *Awakening* conditions across brain regions/networks. The blue underlay marks the reduced distribution range across regions on awakening.

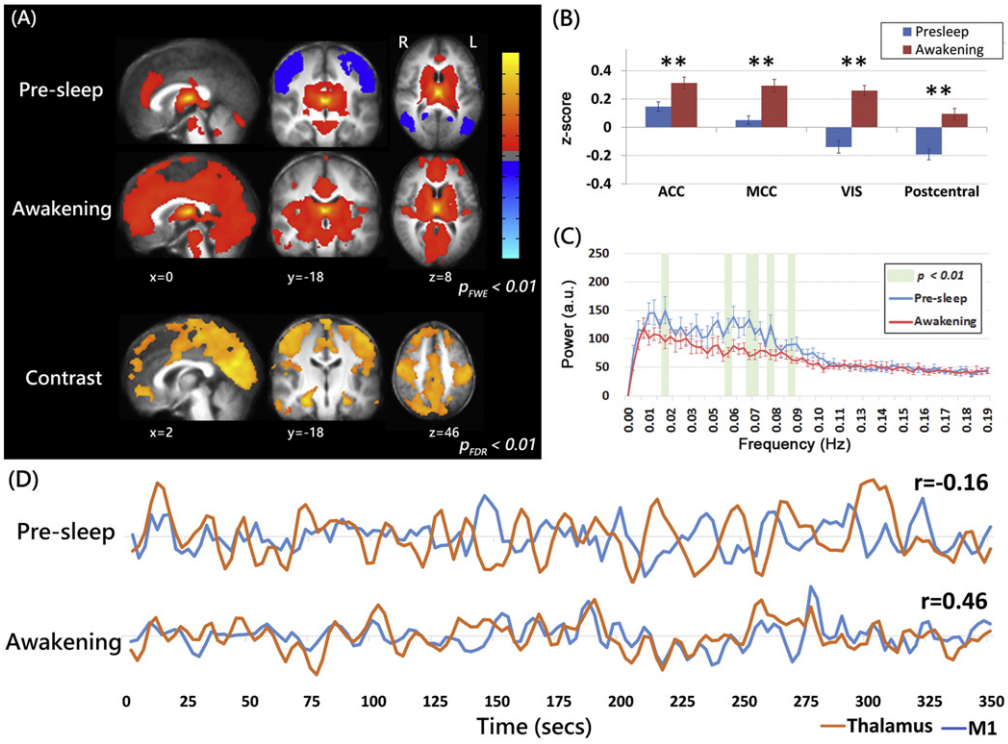


**Fig. 3.** Comparison of thalamo-cortical connectivity and thalamus dynamics between *Pre-sleep* and *Awakening*. (A) Thalamo-cortical connectivity maps of one-sample in *Pre-sleep* and *Awakening* (upper and middle panel, FWE-corrected $P < .01$) and paired comparison (lower panel, FDR-corrected $P < .01$). (B) ROI-based connectivity comparison between *Pre-sleep* (blue) and *Awakening* (red) conditions (**$P < .01$). (C) The thalamus spectral comparison between *Pre-sleep* (blue) and *Awakening* (red) sessions. The error bar shows the between-subject variation and the green underlay denotes the frequency bands with significant difference (paired t-test, $P < .01$). (D) Temporal demonstration of the fluctuation amplitude and synchronization between the thalamus (orange) and the primary motor cortex (blue) were extracted from *Pre-sleep* and *Awakening* sessions.

observable frequency range), AG (0.03 Hz), MT (0.03, 0.045 and 0.15 Hz) and THA (0.15–0.16 Hz and 0.19 Hz), but did not present notable changes in ACC and HPC. In contrast, the light-sleep group power spectra across ROIs remained stable. It only presented reduced power density in PCC (0.05 Hz) and VIS (0.04–0.08 Hz), while ACC (0.18 Hz) and AG (0.12 Hz) had slight increased power on awakening.

Inline Supplementary Fig. S2 can be found online at http://dx.doi.org/10.1016/j.neuroimage.2014.07.032.

## Discussion

Echoing the local sleep notion, the local awakening hypothesis was firstly addressed and tested by RS-fMRI techniques. We demonstrated that brain oscillations were regionally regulated on awakening and affected by sleep architecture. Reduced sensorimotor connectivity indicated poor sensorimotor performance on awakening, whereas the enhanced thalamo-cortical connectivity suggested a plausible sleep–waking regulation function of the thalamus and perception refreshment. In the frequency domain, overall reduced low-frequency power implied energy preservation during sleep. Considering the stage effect, functional connectivity and spectral reduction were dependent on the existence of N3 sleep before waking. These results indicated a general sleep regulation of brain oscillations on awakening and supported the local awakening hypothesis. Besides, in the current work, we focused on the local changes of brain networks upon awakening by means of fMRI. The corresponding EEG data were also collected but not reported here due to the following concerns: (1) Modern EEG–fMRI techniques assume a stable hemodynamic function; however, such assumption may be invalid across physiological conditions. The direct linkage between EEG and fMRI may be controversial due to the undetermined neurovascular couplings regulated by sleep, which is beyond the scope of the current study. (2) Uncertainty exists in co-registering the spatial locations of EEG channels and fMRI voxels, especially for deep brain regions. (3) The spectral correspondence between EEG and fMRI is not fully understood. Even though, the inclusion of both EEG and fMRI will be essentially useful to unveil the brain oscillations during sleep and upon awakening, after solving the technical considerations between neuroimaging modalities.

### *Functional connectivity variations on awakening*

Following globally reduced spectral power after sleep, the variations of functional connectivity patterns were specific to brain networks, consistent with the local awakening concept. Studies have suggested the association of the DMN with the cognitive function of internal awareness and declarative memory (Boly et al., 2007; Yan et al., 2009); specifically during NREM sleep, the dissociation of DMN components reflects sleep-induced consciousness suspension (Horovitz et al., 2009; Sämann et al., 2011). Based on the DMN decoupling in sleep, our results showed that the DMN components were intact in both *Pre-sleep* and *Awakening* conditions, suggesting the prompt recovery of DMN connectivity and self-awareness within 6 min following wakefulness. We observed a similar enhanced connectivity between bilateral hippocampi, implying the fast recovery of memory-associated functions. However, recovery of low-level cognitive networks might not be as fast as that of high-order ones. The prominently reduced SMN connectivity after sleep indicated the sleep inertia effect (Tassi and Muzet, 2000), and that bilateral connections were recovered within 30 min. Similarly, the dissociation of M1 and SMA following the fatigue task may explain short-term clumsiness and sluggish behavior immediately after sleep (Peltier et al., 2005). The current report provides fMRI-based measurements to evaluate the cognitive influence of sleep disorders objectively, particularly for obstructive sleep apnea and narcolepsy.

The thalamus is composed of a set of nuclei, containing neurons that relay perceptual information from external environments in wakefulness (Hughes et al., 2011). In sleep, the midline and intralaminar nuclei

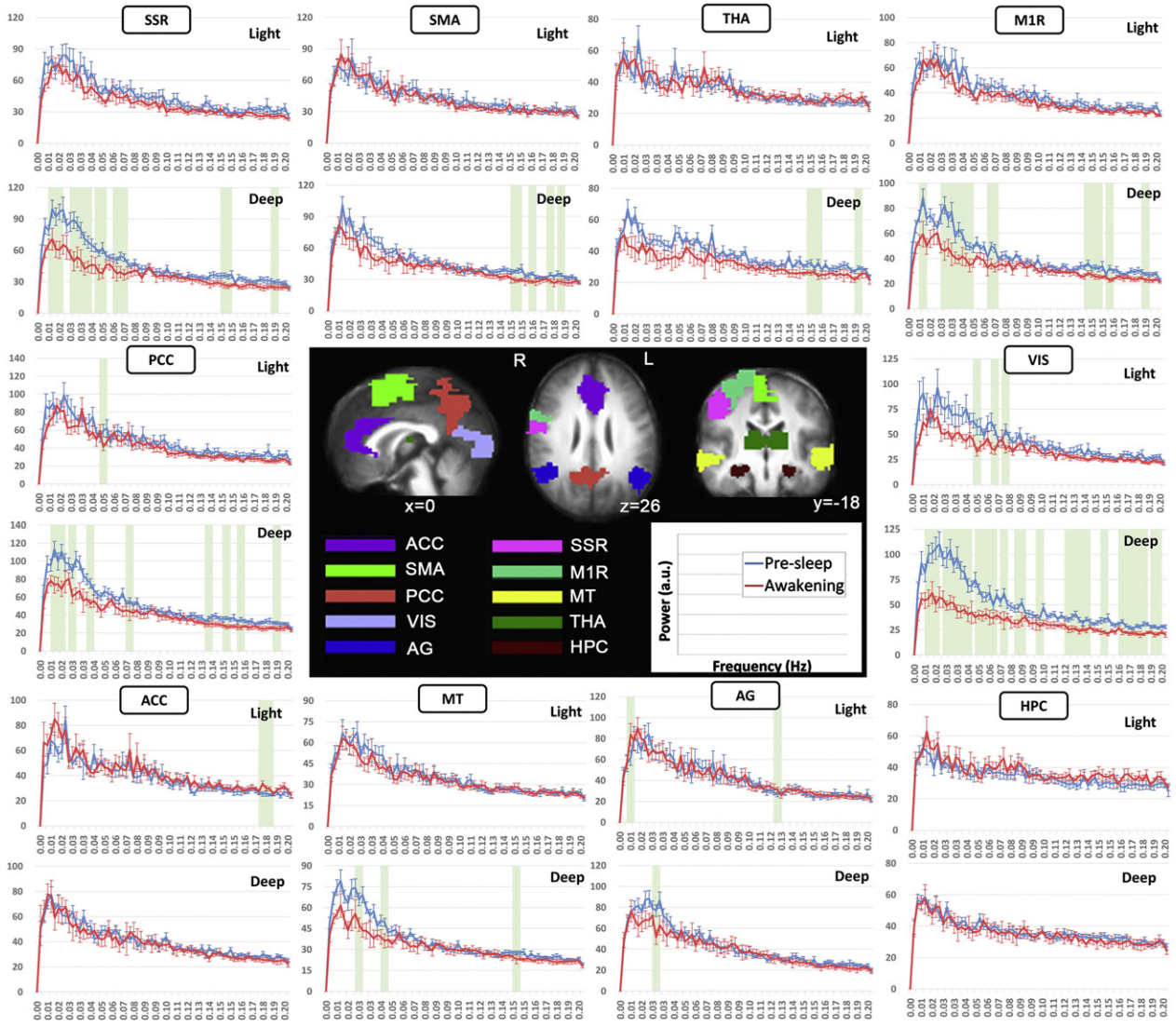


**Fig. 4.** Stage effect on the spectral power of light-sleep (upper panel, without N3 sleep) and deep-sleep groups (lower panel, with N3 sleep) across AAL regions. The paired comparison between *Pre-sleep* (blue) and *Awakening* (red) conditions was performed on spectral power in the 10 representative ROIs: postcentral sensory area (SSR), supplementary motor area (SMA), thalamus (THA) right primary motor cortex (M1R), posterior cingulate cortex (PCC), the calcarine visual area (VIS), anterior cingulate cortex (ACC), middle temporal cortices (MT), angular gyri (AG), and hippocampus (HPC). The light-green background indicates the significance level of $P < .01$ (paired t-test, two-tailed).

of the thalamus play a critical gating role in thalamocortical transmission by preventing relay neurons from being hyperpolarized and entering into burst mode, thereby blocking the means for thalamo-cortical sensory transmission (Halassa, 2011). Previous imaging studies showed that thalamo-cortical dynamics may be desynchronized during loss of consciousness (Boveroux et al., 2010; Zhou et al., 2011); similarly, the most robust findings in this study were the pervasive enhancements of thalamo-cortical connectivity on awakening. In contrast, the thalamo-cortical connectivity before sleep appeared relatively desynchronous (Fig. 3A), presenting positive correlations only to the MCC/cerebellum and its negative connection to SMN. The negative connectivity arose from an obvious phase delay between M1 and THA (Fig. 3D), implying the inefficiency of transferring temporal dynamics from the thalamus to the perceptual system. After leaving the burst mode and recovering from sleep, thalamo-cortical connectivity may be re-established by reducing the temporal delays to the entire neo-cortex, leading to the refreshed sensation after sleep. Beyond the cortico-cortical relay functions, the thalamus may act as the consciousness switch, leading to cortical arousal. Scientists conducting propofol-induced unconsciousness in humans have observed decreased thalamocortical connections following the depth of unconsciousness levels and suggested that the medial thalamus is related to vigilance and external conscious perception (Boveroux et al., 2010; Guldenmund et al., 2013). These investigations support our findings of connectivity changes after sleep and elucidate the importance of thalamo-cortical interactions during sleep. Consequently, we provide alternative evidence for consciousness recovery by observing the local awakening of the thalamo-cortical network.

### *Physiological changes of BOLD fluctuations on awakening*

Unlike the multiple combinations of seed-correlation analysis, the univariate spectral power of the RS-fMRI signal provides higher sensitivity to cerebral physiology and psychiatric disorders (Han et al., 2011; Yu et al., 2014). Recent studies have suggested that BOLD signal temporal fluctuations reflect cortical neuronal activity, vigilance level, and the development process (McIntosh et al., 2010; Pelled and Goelman, 2004). In the current study, we observed an overall decreased ALFF on awakening, but only the posterior brain (parietal and occipital lobes) showed significant reductions in the voxel-wise comparison (Fig. 2A upper panel), indicating that the anterior brain (frontal lobe and limbic system) maintains equal or slightly higher ALFF on awakening. The ALFFn maps (Fig. 2A lower panel) illustrated an imagery

separation line extending from the brain stem to the central sulcus, where the brain area anterior to this line possessed sustained or elevated spectral power on awakening and the posterior part showed decreased power. The ALFFn results matched the previous findings in the spatial extent, which reported fast rCBF re-establishments in anterior brain regions after sleep (Balkin et al., 2002). These reports partially supported the speculation that fMRI spectral variance has physiological implications originating from rCBF, but further analysis is required to disclose the physiological mechanisms of baseline fMRI fluctuations.

We addressed the ROI-based spectral analysis to specify the frequency bins sensitive to the changes between *Pre-sleep* and *Awakening* conditions. Most power distribution changes were contained within 0.01 to 0.07 Hz in the cortical area (Fig. 4) and within a wider range of 0.05 to 0.09 Hz in the medial thalamus (Fig. 3C). Although low-frequency power is not fully understood in the fMRI signal, studies have provided corresponding electrophysiological evidence on awakening. Ferrara and colleagues characterized a pattern of increased EEG power in the delta–theta bands with decreased beta power of the awakening brain (Ferrara et al., 2006). Marzano further elucidated that the awakening variation of delta power was regional specific (delta enhancement in the posterior brain and delta reduction in the frontal lobe), whereas beta power was globally decreased on awakening (Marzano et al., 2011). Our results indicated that the global reduction of ALFF resembling reduced beta power from the Marzano observation; however, the anterior/posterior ALFFn disparities were reversely proportional to delta power increases. Such results seemed incongruent with each other; however, an earlier study estimating rCBF and delta wave using positron emission tomography reported that the interaction between rCBF and delta activity was opposite between frontal and posterior regions during sleep (Hofle et al., 1997), which provides another clue to explain the complex findings of neurovascular coupling. In short, the changes of regional physiologies revealed recovered top-down coordination in the anterior brain but silent bottom-up sensory coordination in the posterior brain, immediately upon awakening.

*Interactions between spectral power and functional connectivity*

Spectral power and functional connectivity are two different measures of examining the amplitudes and phases of temporal dynamics, and may provide more understanding of the dynamic changes of brain networks. *Inline Supplementary Fig. S3* delineates the general observations of the 4 networks on awakening. For the local awakening notion, we speculated 3 inferences from our study scenarios. First, reduced spectral power with reduced connectivity in the perceptual networks, such as SMN and visual networks, implying restored energy during sleep to preserve hemodynamic perturbations. Under such circumstances, these networks lost temporal dynamics (frequency range: 0.01–0.07 Hz and 0.15–0.16 Hz in SMN) responsible for bilateral synchronizations on awakening. Second, sustained spectral power with enhanced/sustained connectivity in high-order cognitive networks, such as HPN and DMN, indicated that the temporal dynamics of these networks were re-synchronized to be in-phase after sleep, although spectral power distribution was unaffected. The dynamic processes from desynchronization to re-synchronization may be the key issue toward the refreshed feeling following wakefulness. Third, reduced spectral power with enhanced connectivity was presented in the thalamo-cortical dialogue, implying that the temporal dynamics specific to 0.05–0.09 Hz serve as a factor disturbing thalamo-cortical connectivity. Such a disturbing factor may resemble the theta power associated with sleep pressure (Borbély and Achermann, 1999), and intrigue the sleep onset. However, we raised these inferences from current observations based on spectral distribution and functional connectivity changes, which require further investigations for validation based on non-stationarity.

Inline Supplementary Fig. S3 can be found online at http://dx.doi.org/10.1016/j.neuroimage.2014.07.032.

*Stage effects of BOLD oscillations on awakening*

Local awakening hypothesized that sleep architectures before awakening affect brain dynamics on awakening. To test the hypothesis, we applied connectivity and spectral analyses to both light-sleep ($N = 10$) and deep-sleep ($N = 12$) groups. Although within-group comparisons showed significant connectivity changes after sleep, the between-group comparisons did not present significant differences ($P > .3$). This observation could be due to the insufficient sample size and low sensitivity in the voxel-based comparison, the between-group connectivity could not reach the significance confidence level due to lack of degree of freedom. On the other hand, in SMA, HPC, and the visual area, spectral disparity was only prominent in the deep-sleep group, affecting extra-low frequency in HPC/SMA and broad bands in the visual area. Reduced spectral power may reflect the residual effect of slow-wave propagation that forms memory consolidation and restored perceptions (Mignot, 2008; Nir et al., 2011). In ACC, we observed elevated spectral power (0.18–0.19 Hz, out of the typical observation range in RS-fMRI analysis) in the light-sleep group. Because ACC partially belongs to the emotional network, such results implied stabilized SWS brain dynamics, particularly for regulating emotions (Gujar et al., 2011). In contrast to light-sleep, PCC and THA possessed stronger spectral reduction in deep-sleep; however, it did not reach the significance level because of the insufficient sample size. The other interesting finding of ROI-based spectral analysis was that across most regions in Fig. 4, the *Pre-sleep* spectral power in deep-sleep group was significantly higher than that in other levels. Since the two groups had no significant difference in sleep scoring (Inline Supplementary Table S2), this phenomenon leads to the implication that lowering the enhanced BOLD spectral power to a baseline level was one of the functions of slow-wave sleep, especially in the low-level sensory systems. Such rebooting process is similar to the alleviation of sleep pressure in previous electrophysiological studies (Vyazovskiy et al., 2011; Hung et al., 2013), providing more spatial information to survey the regional specificity. Once again, to understand the underlying mechanisms on the fMRI findings, disentangling the complex coupling between electrical and hemodynamic activities would be crucial before stepping forward.

*Limitations*

When we conducted the functional scans at midnight, both *Pre-sleep* and *Awakening* sessions were with enhanced sleep pressure, different from the normal awake resting state. Although NREM sleep occurs in the *Pre-sleep* session, previous sleep neuroimaging literature indicated that the disparities of functional connectivity and spectral power between N1/N2 sleep and pre-sleep resting condition were minimal and negligible, but the disparity emerged in N3 sleep (Larson-Prior et al., 2009; Sämann et al., 2011). Besides, previous EEG studies demonstrated that the sleep pressure increased the alpha to theta waves in the awakening brain before sleep (Taillard et al., 2003), where such micro-sleep raises the false-alarm chance to be scored into sleep stages. Therefore, we regarded that these confounding factors might slightly affect the conditions, but did not conflict with the overall sleep regulation effects on the awakening brain. An alternative concern is that the results of higher spectral reduction in deep sleep group (Fig. 4) may come from more NREM sleep in *Pre-sleep* session of deep sleep group. To this point, we first analyzed the sleep scoring for both groups and found that there was no significant difference in NREM sleep between groups in the *Pre-sleep* session ($P > .32$). Secondly, Sämann et al (2011) indicated that in wakefulness, only high frequency band (0.10–0.15 Hz) possessed significantly stronger BOLD spectral power than N1/N2 sleep. In our results, we compositely found that the significant spectral changes were majorly located in the low-frequency range (0.01–0.08 Hz), and only prominent in deep sleep group. All together, the occasional NREM sleep in the *Pre-sleep* session minimally affected our connectivity and spectrum findings. Practically speaking, using the 'open-eye' instruction

for the resting-state scan in the midnight is preferred to avoid the sleepiness when closing the eyes.

Distinguishing the origins of brain variability on awakening was arduous under our experimental design because of the single measurement after sleep. Reduced fluctuations and increased connectivity could be a successive and stable influence to functional networks on awakening (sleep restoration effect), or a transient and unstable phenomenon after sleep (sleep inertia effect). Electrophysiological investigations on awakening have focused on prolonged sleep inertia effects for approximately half an hour that returned to normal (Ikeda and Hayashi, 2008; Tassi and Muzet, 2000). However, the long-term sleep restoration effect may be effective because studies support that fMRI connectivity is modulated by circadian rhythms (Blautzik et al., 2013). Because sleep restoration may be associated with subsequent cognitive functions, cerebral changes on awakening require further clarification. Simultaneous recordings of EEG and fMRI were necessary methods for conducting the neuroimaging-based sleep experiments. However, under the constraints of MRI space and the limitation of maximum scan measurements, the sleeping experiments only allowed a 2-h span. Although the 2-h duration was sufficient to record the first sleep cycle, the special MRI environment might cause participant discomfort or the inability to fall sleep. Therefore, we requested the participants to become accustomed to the MR scanning environment the day before conducting the sleep experiment. Improvements for the sleep environment would further benefit the sleep experience inside the scanner, prolong the sleep duration, and increase the sample size.

## Conclusion

The local awakening hypothesis was firstly addressed with two aspects toward the functional reorganization upon awakening: regional specificity and regulation by previous sleep stages. Based on the high spatial resolution of RS-fMRI techniques, we concluded that both functional connectivity and spectral power on awakening were regulated by the sleep architecture across multiple brain networks, supporting the local awakening concept. Additionally, the spectral power reduction on awakening also demonstrated the regional specificity of frequency variations, which may be linked to the rebooting process of sleep pressure. Technically, the multi-dimension analyses using spectrum and connectivity endorsed the internal maintenance process reflected in spontaneous BOLD fluctuations and provided a novel strategy to disclose the brain connectivity under multiple physiological conditions.

## Significance statement

The local awakening hypothesis was firstly addressed with two aspects toward the functional reorganization upon awakening: regional specificity and regulation by previous sleep stages. To test the hypothesis, we performed RS-fMRI analyses on functional connectivity and spectral power. We found that both functional indices were regulated across multiple brain networks on awakening, supporting the local awakening concept. Additionally, the spectral power reduction on awakening also demonstrated the regional specificity of frequency variations, which could be linked to the rebooting process of cognitive functions and sleep pressure.

## Acknowledgments

This research was supported by the Ministry of Science and Technology (MOST 102-2320-B-008-003, MOST 102-2911-I-008-001 and MOST 102-2511-S-008-004).

## References

Adam, K., Oswald, I., 1977. Sleep is for tissue restoration. J. R. Coll. Physicians Lond. 11, 376–388.

Aserinsky, E., Kleitman, N., 1953. Regularly occurring periods of eye motility, and concomitant phenomena, during sleep. Science 118, 273–274.

Balkin, T.J., Braun, A.R., Wesensten, N.J., Jeffries, K., Varga, M., Baldwin, P., Belenky, G., Herscovitch, P., 2002. The process of awakening: a PET study of regional brain activity patterns mediating the re-establishment of alertness and consciousness. Brain 125, 2308–2319.

Biswal, B., Yetkin, F.Z., Haughton, V.M., Hyde, J.S., 1995. Functional connectivity in the motor cortex of resting human brain using echo-planar MRI. Magn. Reson. Med. 34, 537–541.

Biswal, B.B., Pathak, A.P., Ulmer, J.L., Hudetz, A.G., 2003. Decoupling of the hemodynamic and activation-induced delays in functional magnetic resonance imaging. J. Comput. Assist. Tomogr. 27, 219–225.

Blautzik, J., Vetter, C., Peres, I., Gutyrchik, E., Keeser, D., Berman, A., Kirsch, V., Mueller, S., Pöppel, E., Reiser, M., Roenneberg, T., Meindl, T., 2013. Classifying fMRI-derived resting-state connectivity patterns according to their daily rhythmicity. NeuroImage 71, 298–306.

Boly, M., Balteau, E., Schnakers, C., Degueldre, C., Moonen, G., Phillips, C., Peigneux, P., Maquet, P., Laureys, S., 2007. Baseline brain activity fluctuations predict somatosensory perception in humans. Proc. Natl. Acad. Sci. U. S. A. 104, 12187–12192.

Borbély, A.A., Achermann, P., 1999. Sleep homeostasis and models of sleep regulation. J. Biol. Rhythm. 14, 557–568.

Boveroux, P., Vanhaudenhuyse, A., Bruno, M.-A., Noirhomme, Q., Lauwick, S., Luxen, A., Degueldre, C., Plenevaux, A., Schnakers, C., Phillips, C., Brichant, J.-F., Bonhomme, V., Maquet, P., Greicius, M.D., Laureys, S., Boly, M., 2010. Breakdown of within- and between-network resting state functional magnetic resonance imaging connectivity during propofol-induced loss of consciousness. Anesthesiology 113, 1038–1053.

Cox, R.W., 1996. AFNI: software for analysis and visualization of functional magnetic resonance neuroimages. Comput. Biomed. Res. 29, 162–173.

Dang-Vu, T.T., Schabus, M., Desseilles, M., Sterpenich, V., Bonjean, M., Maquet, P., 2010. Functional neuroimaging insights into the physiology of human sleep. Sleep 33, 1589–1603.

Edgar, D.M., Dement, W.C., Fuller, C.A., 1993. Effect of SCN lesions on sleep in squirrel monkeys: evidence for opponent processes in sleep–wake regulation. J. Neurosci. 13, 1065–1079.

Ferrara, M., Curcio, G., Fratello, F., Moroni, F., Marzano, C., Pellicciari, M.C., Gennaro, L.D., 2006. The electroencephalographic substratum of the awakening. Behav. Brain Res. 167, 237–244.

Gujar, N., Yoo, S.-S., Hu, P., Walker, M.P., 2011. Sleep deprivation amplifies reactivity of brain reward networks, biasing the appraisal of positive emotional experiences. J. Neurosci. 31, 4466–4474.

Guldenmund, P., Demertzi, A., Boveroux, P., Boly, M., Vanhaudenhuyse, A., Bruno, M.-A., Gosseries, O., Noirhomme, Q., Brichant, J.-F., Bonhomme, V., Laureys, S., Soddu, A., 2013. Thalamus, brainstem and salience network connectivity changes during propofol-induced sedation and unconsciousness. Brain Connect. 3, 273–285.

Halassa, M.M., 2011. Thalamocortical dynamics of sleep: roles of purinergic neuromodulation. Semin. Cell Dev. Biol. 22, 245–251.

Han, Y., Wang, J., Zhao, Z., Min, B., Lu, J., Li, K., He, Y., Jia, J., 2011. Frequency-dependent changes in the amplitude of low-frequency fluctuations in amnestic mild cognitive impairment: a resting-state fMRI study. NeuroImage 55, 287–295.

Hayashi, M., Matsuura, N., Ikeda, H., 2010. Preparation for awakening: self-awakening vs. forced awakening preparatory hangs in the pre-awakening period. Int. Rev. Neurobiol. 93, 109–127.

Hofle, N., Paus, T., Reutens, D., Fiset, P., Gotman, J., Evans, A.C., Jones, B.E., 1997. Regional cerebral blood flow changes as a function of delta and spindle activity during slow wave sleep in humans. J. Neurosci. 17, 4800–4808.

Horovitz, S.G., Braun, A.R., Carr, W.S., Picchioni, D., Balkin, T.J., Fukunaga, M., Duyn, J.H., 2009. Decoupling of the brain's default mode network during deep sleep. Proc. Natl. Acad. Sci. U. S. A. 106, 11376–11381.

Hu, P., Stylos-Allan, M., Walker, M.P., 2006. Sleep facilitates consolidation of emotional declarative memory. Psychol. Sci. 17, 891–898.

Huber, R., Felice Ghilardi, M., Massimini, M., Tononi, G., 2004. Local sleep and learning. Nature 430, 78–81.

Hughes, S.W., Lorincz, M.L., Parri, H.R., Crunelli, V., 2011. Infraslow. Prog. Brain Res. 193, 145–162.

Hung, C.-S., Sarasso, S., Ferrarelli, F., Riedner, B., Ghilardi, M.F., Cirelli, C., Tononi, G., 2013. Local experience-dependent changes in the wake EEG after prolonged wakefulness. Sleep 36, 59–72.

Iber, C., 2007. The AASM Manual for the Scoring of Sleep and Associated Events. American Academy of Sleep Medicine, Westchester IL.

Ikeda, H., Hayashi, M., 2008. Effect of sleep inertia on switch cost and arousal level immediately after awakening from normal nocturnal sleep. Sleep Biol. Rhythm. 6, 120–125.

Jung, D.W., Hwang, S.H., Yoon, H.N., Lee, Y.J., Jeong, D.U., Park, K.S., 2014. Nocturnal awakening and sleep efficiency estimation using unobtrusively measured ballistocardiogram. IEEE Trans. Biomed. Eng. 61, 131–138.

Karni, A., Tanne, D., Rubenstein, B.S., Askenasy, J.J., Sagi, D., 1994. Dependence on REM sleep of overnight improvement of a perceptual skill. Science 265, 679–682.

Kuboyama, T., Hori, A., Sato, T., Mikami, T., Yamaki, T., Ueda, S., 1997. Changes in cerebral blood flow velocity in healthy young men during overnight sleep and while awake. Electroencephalogr. Clin. Neurophysiol. 102, 125–131.

Larson-Prior, L.J., Zempel, J.M., Nolan, T.S., Prior, F.W., Snyder, A.Z., Raichle, M.E., 2009. Cortical network functional connectivity in the descent to sleep. Proc. Natl. Acad. Sci. U. S. A. 106, 4489–4494.

Marzano, C., Ferrara, M., Moroni, F., De Gennaro, L., 2011. Electroencephalographic sleep inertia of the awakening brain. Neuroscience 176, 308–317.

Massimini, M., Ferrarelli, F., Huber, R., Esser, S.K., Singh, H., Tononi, G., 2005. Breakdown of cortical effective connectivity during sleep. Science 309, 2228–2232.

McIntosh, A.R., Kovacevic, N., Lippe, S., Garrett, D., Grady, C., Jirsa, V., 2010. The development of a noisy brain. Arch. Ital. Biol. 148, 323–337.
Mignot, E., 2008. Why we sleep: the temporal organization of recovery. PLoS Biol. 6, e106.
Nir, Y., Staba, R.J., Andrillon, T., Vyazovskiy, V.V., Cirelli, C., Fried, I., Tononi, G., 2011. Regional slow waves and spindles in human sleep. Neuron 70, 153–169.
Pelled, G., Goelman, G., 2004. Different physiological MRI noise between cortical layers. Magn. Reson. Med. 52, 913–916.
Peltier, S.J., LaConte, S.M., Niyazov, D.M., Liu, J.Z., Sahgal, V., Yue, G.H., Hu, X.P., 2005. Reductions in interhemispheric motor cortex functional connectivity after muscle fatigue. Brain Res. 1057, 10–16.
Roenneberg, T., 2013. Chronobiology: the human sleep project. Nature 498, 427–428.
Sämann, P.G., Wehrle, R., Hoehn, D., Spoormaker, V.I., Peters, H., Tully, C., Holsboer, F., Czisch, M., 2011. Development of the brain's default mode network from wakefulness to slow wave sleep. Cereb. Cortex 21, 2082–2093.
Song, X.-W., Dong, Z.-Y., Long, X.-Y., Li, S.-F., Zuo, X.-N., Zhu, C.-Z., He, Y., Yan, C.-G., 2011. REST: a toolkit for resting-state functional magnetic resonance imaging data processing. PLoS ONE 6, e25031.
Steriade, M., Timofeev, I., Grenier, F., 2001. Natural waking and sleep states: a view from inside neocortical neurons. J. Neurophysiol. 85, 1969–1985.
Taillard, J., Philip, P., Coste, O., Sagaspe, P., Bioulac, B., 2003. The circadian and homeostatic modulation of sleep pressure during wakefulness differs between morning and evening chronotypes. J. Sleep Res. 12, 275–282.
Tassi, P., Muzet, A., 2000. Sleep inertia. Sleep Med. Rev. 4, 341–353.
Tzourio-Mazoyer, N., Landeau, B., Papathanassiou, D., Crivello, F., Etard, O., Delcroix, N., Mazoyer, B., Joliot, M., 2002. Automated anatomical labeling of activations in SPM using a macroscopic anatomical parcellation of the MNI MRI single-subject brain. NeuroImage 15, 273–289.
van Dijk, K.R.A., Hedden, T., Venkataraman, A., Evans, K.C., Lazar, S.W., Buckner, R.L., 2010. Intrinsic functional connectivity as a tool for human connectomics: theory, properties, and optimization. J. Neurophysiol. 103, 297–321.
Voss, U., 2010. Changes in EEG pre and post awakening. Int. Rev. Neurobiol. 93, 23–56.
Vyazovskiy, V.V., Hanlon, E.C., Cirelli, C., Tononi, G., 2011. Local sleep in awake rats. Nature 472, 443–447.
Walker, M.P., Stickgold, R., 2006. Sleep, memory, and plasticity. Annu. Rev. Psychol. 57, 139–166.
Yan, C., Liu, D., He, Y., Zou, Q., Zhu, C., Zuo, X., Long, X., Zang, Y., 2009. Spontaneous brain activity in the default mode network is sensitive to different resting-state conditions with limited cognitive load. PLoS ONE 4, e5743.
Yang, H., Long, X.-Y., Yang, Y., Yan, H., Zhu, C.-Z., Zhou, X.-P., Zang, Y.-F., Gong, Q.-Y., 2007. Amplitude of low frequency fluctuation within visual areas revealed by resting-state functional MRI. NeuroImage 36, 144–152.
Yu, R., Chien, Y.-L., Wang, H.-L.S., Liu, C.-M., Liu, C.-C., Hwang, T.-J., Hsieh, M.H., Hwu, H.-G., Tseng, W.-Y.I., 2014. Frequency-specific alternations in the amplitude of low-frequency fluctuations in schizophrenia. Hum. Brain Mapp. 35, 627–637.
Zhou, J., Liu, X., Song, W., Yang, Y., Zhao, Z., Ling, F., Hudetz, A.G., Li, S.-J., 2011. Specific and nonspecific thalamocortical functional connectivity in normal and vegetative states. Conscious. Cogn. 20, 257–268.